Experimental evaluation of the twofold electromagnetic enhancement theory of surface-enhanced resonance Raman scattering

Ken-ichi Yoshida,[1,2] Tamitake Itoh,[2,*] Vasudevanpillai Biju,[2] Mitsuru Ishikawa,[2] and Yukihiro Ozaki[1]
[1]*Department of Chemistry, School of Science and Technology, Kwansei Gakuin University, Sanda, Hyogo 669-1337, Japan*
[2]*Nano-Bioanalysis Team, Health Technology Research Center, National Institute of Advanced Industrial Science and Technology (AIST), Takamatsu, Kagawa 761-0395, Japan*

(Received 31 July 2008; revised manuscript received 4 December 2008; published 18 February 2009)

We examined an electromagnetic (EM) theory of surface-enhanced resonance Raman scattering (SERRS) using single Ag nanoaggregates. The SERRS-EM theory is characterized by twofold EM enhancement induced by the coupling of plasmon resonance with both excitation and emission of Raman scattering plus fluorescence. The total emission cross-section spectra of enhanced Raman scattering and enhanced fluorescence were calculated using the following parameters: the spectrum of enhancement factor induced by plasmon resonance, resonance Raman scattering overlapped with fluorescence, and excitation wavelengths. The calculations well agreed with experimental total emission cross-section spectra, thus providing strong indications that the SERRS-EM theory is quantitatively correct.

DOI: 10.1103/PhysRevB.79.085419 PACS number(s): 73.20.−r, 12.20.Fv, 33.20.Fb, 33.80.−b

I. INTRODUCTION

The work of surface-enhanced resonance Raman scattering (SERRS) has recently attracted much attention in analytical science because it has advanced the detection limits of a wide variety of molecules to the single-molecule level.[1–4] Xu and co-workers[4–6] have theoretically demonstrated the single-molecule sensitivity of SERRS based on the SERRS-electromagnetic (EM) theory. This theory is characterized by twofold EM enhancement of Raman scattering and fluorescence of a single molecule contacted with a single metal nanoaggregate; the first enhancement is due to coupling of plasmon resonance with incident light, and the second enhancement is due to coupling of plasmon resonance with Raman-scattering light and fluorescence.[4–10] The twofold EM enhancement theory predicts that a spectrum of total emission of enhanced Raman scattering and enhanced fluorescence will be calculated by the following three parameters: an EM enhancement factor induced by plasmon resonance $M(\lambda_L,\lambda)$, resonance Raman-scattering cross section $\sigma_{\mathrm{RRS}}(\lambda_L,\lambda)$ and fluorescence cross section $\sigma_{\mathrm{FL}}(\lambda_L,\lambda)$, and excitation wavelength λ_L.[4–6]

Variations in plasmon resonance bands of individual Ag nanoaggregates generate widely distributed shapes and intensities of the spectra of EM enhancement factors.[4–15] Ensemble measurements average over the spectra of the EM enhancement factors of individual Ag nanoaggregates and thus prevent us from experimentally testing the SERRS-EM theory. Observation of total emission and plasmon resonance spectra of isolated single silver nanoaggregates makes it possible to experimentally test SERRS-EM theory. Thus, we have measured total emission and plasmon resonance spectra from isolated single Ag nanoaggregates. Spectral shapes of EM enhancement factors of large isolated Ag nanoaggregates are complicated because of overlapping of dipolar and multipolar plasmon resonance bands. To avoid such a complication, we have carefully selected single silver nanoaggregates that show dipolar plasmon resonance.[11–15] Thanks to this careful selection, we have already experimentally demonstrated the evidence for twofold EM enhancement predicted by SERRS-EM theory: (a) coupling of plasmon resonance with incident light,[11–13] and (b) coupling of plasmon resonance with Raman-scattering light plus fluorescence.[14,15] However, the previous work lacks in quantitatively comparing the experimental total emission spectra with those calculated by the SERRS-EM theory by systematically changing the key parameters $M(\lambda_L,\lambda)$, $\sigma_{\mathrm{RRS}}(\lambda_L,\lambda)+\sigma_{\mathrm{FL}}(\lambda_L,\lambda)$, and λ_L, all of which are essential for identification of total emission spectra. The lack of the comparison makes it unclear whether total emission of SERRS and enhanced fluorescence is quantitatively represented using only the three parameters from the SERRS-EM theory. Thus, total emission of SERRS and enhanced fluorescence is recognized as complicated phenomenon.

In the current study we calculated total emission spectra using the SERRS-EM theory, and compared them with experimental total emission spectra by changing three parameters $M(\lambda_L,\lambda)$, $\sigma_{\mathrm{RRS}}(\lambda_L,\lambda)+\sigma_{\mathrm{FL}}(\lambda_L,\lambda)$, and λ_L. The calculated total emission cross-section spectra were quantitatively consistent with experimental total emission cross-section spectra within the framework of the SERRS-EM theory under the current experimental conditions. This consistency provides strong indications that the complex phenomenon such as total emission of SERRS and enhanced fluorescence is quantitatively represented using only the three parameters.

II. EXPERIMENT

A colloidal solution of Ag nanoparticles was prepared following the method of Lee and Meisel.[16] Each NaCl aqueous solution (25 mM) of (i) rhodamine 123 (R123), (ii) rhodamine 6G (R6G), and (iii) rhodamine B (RB) was mixed with an Ag nanoparticle colloidal solution (7.2×10^{-11} M) and incubated for 15 min at room temperature (20 °C). The solution was spin coated on a glass cover slip. Note that the direct use of dye concentration of $\sim10^{-11}$ M in standard single-molecule SERRS experiments caused serious difficulty in finding Ag nanoaggregates showing SERRS activity.

Thus, we initially employed relatively high concentration of the dye ($\sim 10^{-8}$ M) to increase the number of Ag nanoaggregates showing SERRS activity. Then, we reduced effective concentration of the dye in the following two steps. First, we completely rinsed away most of the dye molecules adsorbed on both silver nanoaggregates and glass surfaces with acetone and water.[15] Second, we found that the spectral shape and intensity of both SERRS and background light became quantitatively similar to the ones using dye concentration ($\sim 10^{-11}$ M). We also found that fluorescence signals were never detected from glass surfaces. From the above steps, we assumed that effective dye concentration of the current experiments is almost equivalent to that of single-molecule SERRS ones.

The details of the spectroscopic setup were described elsewhere.[11] Briefly, a 100 W halogen lamp through a dark-field condenser lens was used as a white-light source to measure plasmon resonance spectra. An Ar^+ laser (514 nm, 2 W/cm^2) and a Kr^+ laser (568 nm, 2 W/cm^2; 647 nm, 2 W/cm^2) were used for total emission excitation. Spectra of total emission intensity $I_T(\lambda_L,\lambda)$ (photocounts) and plasmon resonance-scattering intensity $I_p(\lambda_L,\lambda)$ (photocounts) were converted into the cross-section spectra of total emission $\sigma_T(\lambda_L,\lambda)$ (cm^2) and those of plasmon resonance scattering $\sigma_p(\lambda_L,\lambda)$ (cm^2) using a 80 nm gold nanosphere, whose scattering intensity and scattering cross section are known. Note that the conversion factor for total emission is 2.3×10^{-18} (cm^2/photocounts) and the conversion factor for plasmon resonance scattering is 2.3×10^{-18} (cm^2/photocounts) on the current spectroscopic equipment.

III. RESULTS AND DISCUSSION

The total emission cross-section spectrum $\sigma_T(\lambda_L,\lambda)$ is written as the sum of an enhanced resonance Raman-scattering cross-section spectrum $\sigma_{\mathrm{ERRS}}(\lambda_L,\lambda)$ and an enhanced fluorescence cross-section spectrum $\sigma_{\mathrm{EFL}}(\lambda_L,\lambda)$ because both cross-section spectra are simultaneously enhanced by plasmon resonance within the framework of the SERRS-EM theory.[5,6] Thus,

$$\sigma_T(\lambda_L,\lambda) = \sigma_{\mathrm{ERRS}}(\lambda_L,\lambda) + \sigma_{\mathrm{EFL}}(\lambda_L,\lambda). \tag{1}$$

An EM enhancement factor spectrum $M(\lambda_L,\lambda)$ is a product of first and second enhancement factors, each of which is induced by coupling of plasmon resonance with incident light and with Raman-scattering light plus fluorescence.[4–7] Note that $M(\lambda_L,\lambda)$ is an enhancement factor of electric-field intensity, not of electric-field amplitude. Thus,

$$M(\lambda_L,\lambda) = \left|\frac{E^{\mathrm{loc}}(\lambda_L)}{E^I(\lambda_L)}\right|^2 \times \left|\frac{E^{\mathrm{loc}}(\lambda)}{E^I(\lambda)}\right|^2 = M_1(\lambda_L)M_2(\lambda), \tag{2}$$

where E^I and E^{loc} indicate the amplitude of a far field and a local field, respectively. The factors $M_1(\lambda_L)$ and $M_2(\lambda)$ are spectra of the first and second enhancement factors, respectively. Thus,

$$\sigma_{\mathrm{ERRS}}(\lambda_L,\lambda) = M_1(\lambda_L)M_2(\lambda)\sigma_{\mathrm{RRS}}(\lambda_L,\lambda), \tag{3}$$

where $\sigma_{\mathrm{RRS}}(\lambda_L,\lambda)$ is a resonance Raman-scattering cross-section spectrum of a molecule free from surface enhancement. The parameter $\sigma_{\mathrm{EFL}}(\lambda_L,\lambda)$ in Eq. (1) includes a product of EM enhancement of absorption and fluorescence.[5,6] The EM enhancement $M_1(\lambda_L)$ of absorption is equivalent to an increase in effective absorption cross section due to an increase in the incident local-field photon density compared with incident far-field photon density. The plasmon resonance coupled with fluorescence light enhances fluorescence by a factor of $M_2(\lambda)$ and simultaneously quenches fluorescence by a factor of q through energy transfer from a molecule to an Ag nanoaggregate.[5,6] Thus, quenching factor q is multiplied with $\sigma_{\mathrm{FL}}(\lambda_L,\lambda)$ of a molecule free from fluorescence quenching. Thus,

$$\sigma_{\mathrm{EFL}}(\lambda_L,\lambda) = M_1(\lambda_L)M_2(\lambda)q\sigma_{\mathrm{FL}}(\lambda_L,\lambda). \tag{4}$$

Combining Eqs. (3) and (4) yields[17]

$$\sigma_T(\lambda_L,\lambda) = M_1(\lambda_L)[\sigma_{\mathrm{RRS}}(\lambda_L,\lambda) + q\sigma_{\mathrm{FL}}(\lambda_L,\lambda)]M_2(\lambda). \tag{5}$$

Now we examine key parameters $M_1(\lambda_L)M_2(\lambda)$, $\sigma_{\mathrm{RRS}}(\lambda_L,\lambda)+q\sigma_{\mathrm{FL}}(\lambda_L,\lambda)$, and λ_L in Eq. (5). The parameter λ_L was simply determined by the lasers we used. Thus, we closely examine the ways to evaluate the parameters $M_1(\lambda_L)M_2(\lambda)$ and $\sigma_{\mathrm{RRS}}(\lambda_L,\lambda)+q\sigma_{\mathrm{FL}}(\lambda_L,\lambda)$. The parameter $M_1(\lambda_L)M_2(\lambda)$ can be Lorentzian:

$$M_1(\lambda_L)M_2(\lambda) \propto 1/[(1/\lambda_P - 1/\lambda)^2 + \Gamma^2], \tag{6}$$

where λ_P is the wavelength of plasmon resonance maximum while Γ is the linewidth inversely proportional to the dephasing time. Because we selected Ag nanoaggregates showing dipolar plasmon resonance whose spectral maxima are in the region of 550–650 nm, the radiation damping parameter $1/\Gamma$ in this spectral region dominates dephasing of the plasmon oscillation. Thus, a plasmon resonance band will be Lorentzian.[18,19] Here, λ_P and Γ in a Lorentzian band shape in Eq. (6) were assumed to be equal to those in an experimental plasmon resonance band.

We provide clues to accept the above assumption as follows. Basically, $M_1(\lambda_L)M_2(\lambda)$ and plasmon resonance Rayleigh scattering are originated from plasmons.[4–7,10] Thus, we can understand the similarity in spectra between $M_1(\lambda_L)M_2(\lambda)$ and plasmon resonance Rayleigh scattering. Indeed, near field scanning optical microscopy using single gold nanoparticles provides the evidence for the similarity.[20] However, whether this experimental evidence is applicable to $M_1(\lambda_L)M_2(\lambda)$ at junctions of SERRS-active nanoaggregates is unknown. To resolve the above issue, we have examined $M_1(\lambda_L)M_2(\lambda)$ and plasmon resonance Rayleigh scattering spectra of single silver nanoaggregates. We carefully selected single silver nanoaggregates that show dipolar plasmon resonance bands in plasmon resonance Rayleigh scattering spectra. Thanks to this careful selection, we found that polarization dependence of the dipolar plasmon resonance bands is the same as that of SERRS.[11] From the common polarization dependence, we identified the dipolar plasmon resonance that causes SERRS.[13] Furthermore, we compared

$$\sigma_{SERRS}(\lambda_L,\lambda) = [\sigma_{RRS}(\lambda_L,\lambda) + q \times \sigma_{FL}(\lambda_L,\lambda)]\, M_1(\lambda_L)M_2(\lambda)$$

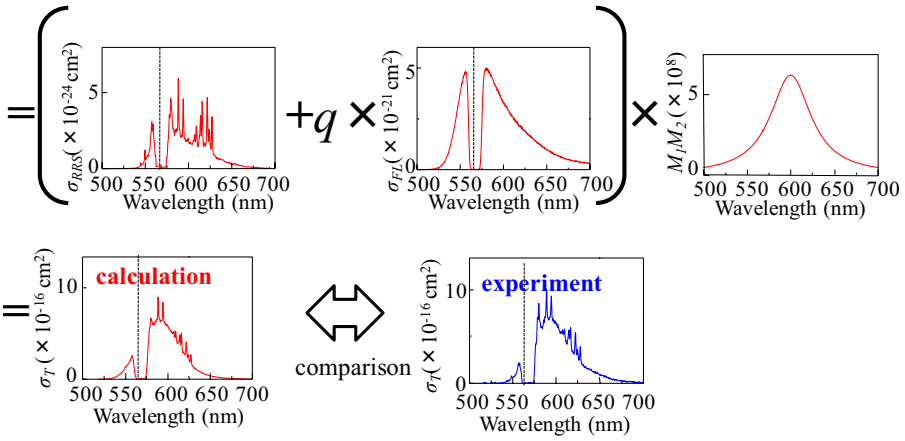

FIG. 1. (Color online) Graphical presentation of quantitative evaluation of total emission spectra.

the spectral shapes of plasmon resonance Rayleigh scattering with those of SERRS. From the comparison, we found that the product of Raman-scattering spectrum and plasmon resonance Rayleigh scattering spectrum well reproduces SERRS spectral shape.[14] The reproduction verifies that the spectral shape of $M_1(\lambda_L)M_2(\lambda)$ is almost equal to that of the plasmon resonance Rayleigh scattering. The similarity of a plasmon resonance Rayleigh scattering band with a $M_1(\lambda_L)M_2(\lambda)$ is confirmed by finite difference time domain (FDTD) calculation using dimers of Ag nanoparticles.[21] We also obtained FDTD calculations (data not shown) similar to those in Ref. 21. From the above rationale, we safely assume that spectral shape of $M_1(\lambda_L)M_2(\lambda)$ is the same as that of plasmon resonance Rayleigh scattering in the current work. Thus, we obtained a Lorentzian band $M_1(\lambda_L)M_2(\lambda)$ including assumed λ_P and Γ, and calculated $\sigma_T(\lambda_L,\lambda)$ using this assumed Lorentzian band. Note that the maximum value of an assumed Lorentzian band in Eq. (6) is a fitting parameter to make the calculated $\sigma_T(\lambda_L,\lambda)$ consistent with experimental $\sigma_T(\lambda_L,\lambda)$. The numerical validity of the maximum value of $M_1(\lambda_L)M_2(\lambda)$ will be discussed later.

The parameter $\sigma_{\mathrm{RRS}}(\lambda_L,\lambda)+q\sigma_{\mathrm{FL}}(\lambda_L,\lambda)$ is composed of two experimental parameters: $\sigma_{\mathrm{RRS}}(\lambda_L,\lambda)$ and $\sigma_{\mathrm{FL}}(\lambda_L,\lambda)$, and one fitting parameter q. However, $\sigma_{\mathrm{RRS}}(\lambda_L,\lambda)$ cannot directly be obtained by experiment because strong fluorescence disturbs us to observe $\sigma_{\mathrm{RRS}}(\lambda_L,\lambda)$ of fluorescent dye molecules; also $q\sigma_{\mathrm{FL}}(\lambda_L,\lambda)$ on a single Ag nanoaggregate without EM enhancement cannot be directly observed.[6] The Stokes resonance Raman spectrum of R6G was observed by removing strong fluorescence using a Kerr shutter.[22] However, low resolution and only the Stokes region of the resonance Raman spectrum thus observed does not meet the current requirement of the calculation. To resolve the issue of the low resolution and the limited spectral region, we obtained $\sigma_{\mathrm{RRS}}(\lambda_L,\lambda)$ from the high-resolution Stokes SERRS spectrum of an ensemble of Ag nanoaggregates that we measured. We have already found that the spectral shape of plasmon resonance of the ensemble Ag nanoaggregates was flat due to the sum of many plasmon resonance spectra whose spectral maxima are different from Ag aggregate to aggregate and randomly distributed in the Stokes region.[14,23] Thus, the spectral shapes of $M_1(\lambda_L)M_2(\lambda)$ of ensemble Ag nanoaggregates are also flat. For this reason, each spectral line within a Stokes SERRS of an ensemble Ag nanoaggregate will be uniformly enhanced and the shape of the SERRS spectrum becomes the same as that of a resonance Raman spectrum. Indeed, the Stokes SERRS spectrum of an ensemble Ag nanoaggregate is equivalent to a resonance Raman spectrum.[22] Thus, we used Stokes SERRS spectra of ensemble Ag nanoaggregates adsorbed by each dye as Stokes resonance Raman-scattering spectra. An anti-Stokes Raman-scattering spectrum was calculated using the Stokes SERRS spectrum thus obtained taking the Boltzmann distribution and an effect of resonance enhancement into account.[24,25] Thus, we obtained the total parameter $\sigma_{\mathrm{RRS}}(\lambda_L,\lambda)$ by combining the experimental Stokes and the calculated anti-Stokes spectra. Note that the unit of $\sigma_{\mathrm{RRS}}(\lambda_L,\lambda)$ (photocount) thus obtained is converted into the cross section (cm^2) using a calculated Raman profile $\sigma_R(\lambda_L,\lambda)$ of a rhodamine molecule.[6] The Raman profile shows excitation-wavelength dependence of Raman spectra. A fluorescence spectrum of each rhodamine molecule in an aqueous solution was substituted for the parameter $\sigma_{\mathrm{FL}}(\lambda_L,\lambda)$ because the electronic state of rhodamine molecules physically adsorbed on an Ag surface is equivalent to that in the solution.[26,27] The unit of $\sigma_{\mathrm{FL}}(\lambda_L,\lambda)$ (photocounts) is converted into cross section (cm^2) using an absorption cross-section spectrum $\sigma_{\mathrm{ABS}}(\lambda_L,\lambda)$ derived from Lambert-Beer's law and fluorescence quantum efficiency of R123, R6G, and RB (0.9, 0.95, and 0.70, respectively). The fitting parameter q was evaluated to make calculated $\sigma_T(\lambda_L,\lambda)$ consistent with experimental $\sigma_T(\lambda_L,\lambda)$. Thus, we obtained $\sigma_{\mathrm{RRS}}(\lambda_L,\lambda)+q\sigma_{\mathrm{FL}}(\lambda_L,\lambda)$ from the substituted experiments and theoretical calculation. The numerical validity of q will be discussed later. Figure 1 shows the procedures to calculate total emission cross-section spectra and to compare the theoretical total emission cross-section spectra with experimental ones.

Equation (5) includes the three parameters: $M_1(\lambda_L)M_2(\lambda)$, $\sigma_{\mathrm{RRS}}(\lambda_L,\lambda)+q\sigma_{\mathrm{FL}}(\lambda_L,\lambda)$, and λ_L. To test Eq. (5), changing independently the three parameters will be required. Thus, we calculated total emission spectra using Eq. (5) and compared them with experimental ones in the following three

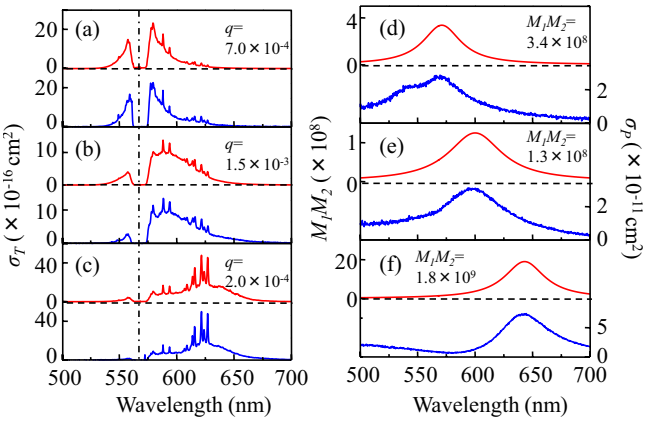

FIG. 2. (Color online) [(a)–(c)] Total emission spectra of R6G calculated by SERRS-EM theory (red lines, upper panels) and experimental total emission spectra (blue lines, lower panels) from three representative nanoaggregates. Total emission spectra were excited at 568 nm. [(d)–(f)] Spectra of $M_1(\lambda_L)M_2(\lambda)$ (red lines) and experimental plasmon resonance Rayleigh scattering spectra (blue lines) from three representative nanoaggregates. Note that left and right axes in (d)–(f) show $M_1(\lambda_L)M_2(\lambda)$ and the cross section of experimental plasmon resonance Rayleigh scattering spectra, respectively. The values of q are inserted in (a)–(c), and the maximum values of $M_1(\lambda_L)M_2(\lambda)$ are inserted in (d)–(f).

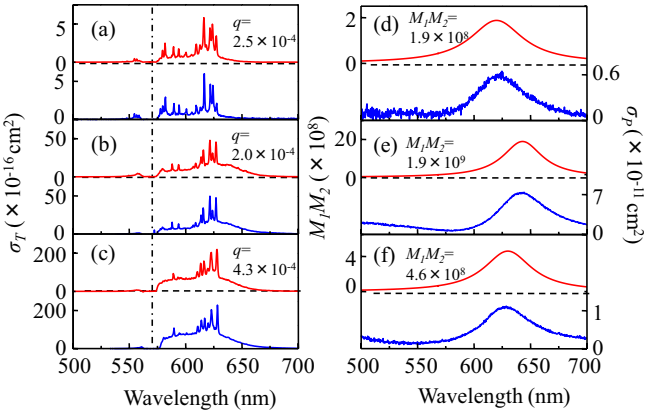

FIG. 3. (Color online) [(a)–(c)] Total emission spectra calculated by SERRS-EM theory (red lines) and experimental total emission spectra (blue lines, excited at 568 nm in a dashed-and-dotted line) of R123, R6G, and RB, respectively. [(d)–(f)] Spectra of $M_1(\lambda_L)M_2(\lambda)$ (red lines, upper panels) and experimental plasmon resonance Rayleigh scattering spectra (blue lines, lower panels). Note that left and right axes in (d)–(f) show $M_1(\lambda_L)M_2(\lambda)$ and the cross section of experimental plasmon resonance Rayleigh scattering spectra, respectively. The values of q are inserted in (a)–(c), and the maximum values of $M_1(\lambda_L)M_2(\lambda)$ are inserted in (d)–(f).

ways, and found consistency between calculations and experiments.

First, total emission spectra from three Ag nanoaggregates with different λ_P and Γ were calculated using Eqs. (5) and (6) for R6G excited at the same λ_L (568 nm). Here, we focus ourselves on the parameter $M_1(\lambda_L)M_2(\lambda)$ characterized by experimental λ_P and Γ in Eq. (6), and associated with each nanoaggregate. In the current calculation, the maximum value of $M_1(\lambda_L)M_2(\lambda)$ and the value of q in $\sigma_{\mathrm{RRS}}(\lambda_L,\lambda)+q\sigma_{\mathrm{EFL}}(\lambda_L,\lambda)$ are fitting parameters. Figures 2(a)–2(c) show three calculated total emission spectra from product of $M_1(\lambda_L)M_2(\lambda)$ and $\sigma_{\mathrm{RRS}}(\lambda_L,\lambda)+q\sigma_{\mathrm{FL}}(\lambda_L,\lambda)$ (red lines; upper panels), and experimental total emission spectra (blue lines, lower panels) of R6G excited at 568 nm. The calculated total emission spectra well describe two characteristics of experimental total emission spectra: (i) the intensity of total emission bands close to the $M_1(\lambda_L)M_2(\lambda)$ maximum is stronger than that in the other regions; (ii) overlapping $M_1(\lambda_L)M_2(\lambda)$ with the fluorescence maximum makes an enhanced fluorescence spectrum dominant in Figs. 2(a) and 2(b), whereas poorly overlapping $M_1(\lambda_L)M_2(\lambda)$ with the fluorescence maximum makes a SERRS scattering spectrum clear in Fig. 2(c). Furthermore, Figs. 2(d)–2(f) show that experimental plasmon resonance spectra (blue lines; lower panels) provided spectral maxima (573, 601, and 643 nm) and bandwidths (40, 55, and 43 nm) similar to those of assumed $M_1(\lambda_L)M_2(\lambda)$ spectra (red lines; upper panels). The similarity shows that plasmon resonance dominates $M_1(\lambda_L)M_2(\lambda)$ spectra. The consistency between calculations and experiments confirms that $M_1(\lambda_L)M_2(\lambda)$ is a key parameter to calculate the total emission spectra using Eq. (5).

Second, total emission spectra were calculated from three Ag nanoaggregates using Eq. (5) for R123, R6G, and RB excited at the same λ_L (568 nm). Note that the values of λ_P and Γ for each Ag nanoaggregate are similar to each other. Here, we focus ourselves on the parameter $\sigma_{\mathrm{RRS}}(\lambda_L,\lambda)+q\sigma_{\mathrm{FL}}(\lambda_L,\lambda)$ characterized by each dye molecule. In the current calculation, the maximum value of $M_1(\lambda_L)M_2(\lambda)$ and the value of q in $\sigma_{\mathrm{RRS}}(\lambda_L,\lambda)+q\sigma_{\mathrm{EFL}}(\lambda_L,\lambda)$ are fitting parameters. Figures 3(a)–3(c) show calculated total emission spectra (red lines; upper panels) and experimental total emission spectra (blue lines; lower panels) of R123, R6G, and RB, respectively. The calculated total emission spectra describe the following two characteristics: (i) the enhanced fluorescence intensity from 580 to 650 nm of R123 in Fig. 3(a) is smaller than that of RB in Fig. 3(c) because the fluorescence maximum of R123 (540 nm) is far from plasmon resonance maxima (630 nm) than that of RB (580 nm); (ii) experimental total emission spectra provide characteristics similar to calculated ones in Fig. 3(a)–3(c). This similarity indicates that the total emission spectra can be determined by product of $M_1(\lambda_L)M_2(\lambda)$ and $\sigma_{\mathrm{RRS}}(\lambda_L,\lambda)+q\sigma_{\mathrm{FL}}(\lambda_L,\lambda)$. Thus, the consistency between the calculated and experimental total emission spectra confirms that $\sigma_{\mathrm{RRS}}(\lambda_L,\lambda)+q\sigma_{\mathrm{FL}}(\lambda_L,\lambda)$ is a key parameter to calculate the total emission spectra using Eq. (5).

Last, total emission spectra were calculated from one Ag nanoaggregate using Eq. (5) for R6G at different λ_L (514, 568, and 647 nm). Here, we focus ourselves on the parameter λ_L characterized by the lasers we used. In the current calculation, the maximum value of $M_1(\lambda_L)M_2(\lambda)$ and the value of q in $\sigma_{\mathrm{RRS}}(\lambda_L,\lambda)+q\sigma_{\mathrm{EFL}}(\lambda_L,\lambda)$ are fitting parameters. Figures 4(a)–4(c) show calculated total emission spectra (red lines; upper panels) and experimental total emission spectra (blue lines; lower panels). Both the calculated and experimental total emission spectra describe the following two characteristics: (i) overlapping a $M_1(\lambda_L)M_2(\lambda)$ maximum with a Stokes Raman spectrum makes a Stokes SERRS dominant in

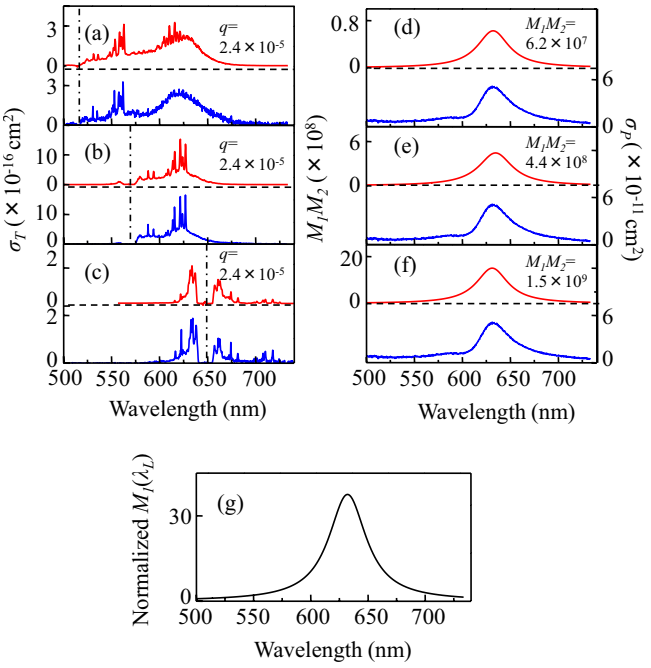

FIG. 4. (Color online) [(a)–(c)] Total emission spectra calculated by SERRS-EM theory (red lines) and experimental total emission spectra (blue lines, excited at 514, 568, and 647 nm in a dashed-and-dotted lines) of R6G. [(d)–(f)] Spectra of $M_1(\lambda_L)M_2(\lambda)$ (red lines) and experimental plasmon resonance Rayleigh scattering spectra (blue lines). Note that left and right axes show $M_1(\lambda_L)M_2(\lambda)$ and the cross section of experimental plasmon resonance Rayleigh scattering spectra, respectively. (g) Wavelength dependence of $M_1(\lambda_L)$. The values of $M_1(\lambda_L)$ are normalized at 514 nm. The values of q are inserted in (a)–(c), and the maximum values of $M_1(\lambda_L)M_2(\lambda)$ are inserted in (d)–(f).

Figs. 4(a) and 4(b) while overlapping a $M_1(\lambda_L)M_2(\lambda)$ maximum with an anti-Stokes SERRS spectrum makes an anti-Stokes SERRS dominant in Fig. 4(c); (ii) the intensity of enhanced fluorescence and SERRS spectra in the region of 620–645 nm in Figs. 4(a)–4(c) is larger than that in the other regions because the $M_1(\lambda_L)M_2(\lambda)$ maximum is located at ~632 nm in Figs. 4(d)–4(f). The above two characteristics are exhibited due to a common $M_1(\lambda_L)M_2(\lambda)$ spectral shape in Figs. 4(a)–4(c). This means that λ_L dependence of total emission spectral shapes is determined by product of $M_1(\lambda_L)M_2(\lambda)$ and $\sigma_{\mathrm{RRS}}(\lambda_L,\lambda)+q\sigma_{\mathrm{FL}}(\lambda_L,\lambda)$. The consistency between the calculated and experimental total emission spectra confirms that λ_L is a key parameter in calculating the total emission spectra using Eq. (5).

Finally, we discuss numerical validity of the two fitting parameters in the current calculation: the maximum value of $M_1(\lambda_L)M_2(\lambda)$ and the value of q. The maximum value of $M_1(\lambda_L)M_2(\lambda)$ used for the calculation in Figs. 2–4 ranges from 6.2×10^7 to 1.9×10^9. The q values used for the calculations in Figs. 2–4 range from 2.4×10^{-5} to 1.5×10^{-3}. The SERRS-EM theory predicts that a dye molecule that locates in an Ag nanoparticle gap within 1.5 nm generates SERRS in the single-molecule sensitivity.[5,6] Maximum values of $M_1(\lambda_L)M_2(\lambda)$ are also estimated to be larger than 6×10^7 for Ag nanoparticles 80 nm in diameter from extended Mie theory.[6] The value of q for such dye is already estimated to be smaller than 2×10^{-2} based on the theory of Förster-type energy transfer.[6] Both the estimated values of $M_1(\lambda_L)M_2(\lambda)$ and q in the previous work[6] are consistent with those derived from the current calculation. The maximum value of $M_1(\lambda_L)M_2(\lambda)$ excited at different λ_L (514, 568, and 647 nm) are different in each other, as shown in Figs. 4(d)–4(f), in spite of the use of the identical Ag nanoaggregate. We consider the origin of this difference in the maximum values. The factor $M_2(\lambda)$ in $M_1(\lambda_L)M_2(\lambda)$ will be common to each $M_1(\lambda_L)M_2(\lambda)$ in Figs. 4(d)–4(f) due to the identical Ag nanoaggregate. Thus, the difference in $M_1(\lambda_L)$ would cause the difference in the maximum value of $M_1(\lambda_L)M_2(\lambda)$. The maximum value of $M_1(\lambda_L)M_2(\lambda)$ in Figs. 4(d)–4(f) is 6.2×10^7, 4.4×10^8, and 1.5×10^9, respectively. The ratio of the maximum value of $M_1(\lambda_L)M_2(\lambda)$ in Fig. 4(d) to that in Figs. 4(d)–4(f) is 1:7:24. Figure 4(g) shows calculated $M_1(\lambda_L)$ factor normalized at 514 nm.[28] The value of $M_1(\lambda_L)$ at 514, 568, and 647 are 1, 3, and 24. Thus, the ratio of the value of $M_1(\lambda_L)$ at 514 nm to that at 568 and 647 nm is 1:3:24. Both the ratios are consistent with each other. The value of q is the same for each λ_L as shown in Figs. 4(a)–4(c) because of the use of the identical Ag nanoaggregate adsorbed with R6G. We consider the reason for the same value of q. The value of q is given by a function of the distance between Ag surfaces and molecules based on the theory of Förster-type energy transfer.[6] The value of q does not change in the measurement of the identical Ag nanoaggregate because the distance between Ag surfaces and molecules is constant.

IV. SUMMARY

In summary the SERRS-EM theory was examined by calculating total emission spectra, independently changing three essential parameters in the theory: EM enhancement factors, Raman plus fluorescence spectra, and excitation wavelengths. Experimental total emission spectra are consistent with the calculated total emission spectra as a function of the three parameters. Furthermore, the calculated SERRS enhancement factors and fluorescence quenching factors are consistent with those in the previous theoretical work. Thus, the twofold consistency demonstrates the SERRS-EM theory. However, this demonstration does not deny the chemical enhancement; that is, optical resonance induced by formation of a charge-transfer (CT) complex increases the molecular Raman-scattering cross section.[29,30] The chemical enhancement is included in the EM theory by exchanging $\sigma_{\mathrm{RRS}}(\lambda_L,\lambda)$ in Eq. (5) with $\sigma_{\mathrm{RRS}}(\lambda_L,\lambda)$ plus cross-section spectrum of CT resonance Raman scattering.

ACKNOWLEDGMENTS

The current work was supported by "Open Research Center" project for private universities, a Grant-in-Aid for Young Scientists (B) (Contract No. 19760041), and Scientific Research (Contract No. 19049013) on Priority Area "Strong Photons-Molecules Coupling Fields (470)" from The Ministry of Education, Culture, Sports and Science and Technology (MEXT) of Japan.

*tamitake-itou@aist.go.jp

[1] K. Kneipp, Y. Wang, H. Kneipp, L. T. Perelman, I. Itzkan, R. R. Dasari, and M. S. Feld, Phys. Rev. Lett. **78**, 1667 (1997).
[2] S. Nie and S. Emory, Science **275**, 1102 (1997).
[3] A. M. Michaels, M. Nirmal, and L. E. Brus, J. Am. Chem. Soc. **121**, 9932 (1999).
[4] H. Xu, E. J. Bjerneld, M. Kall, and L. Borjesson, Phys. Rev. Lett. **83**, 4357 (1999).
[5] H. Xu, X. H. Wang, M. P. Persson, H. Q. Xu, M. Kall, and P. Johansson, Phys. Rev. Lett. **93**, 243002 (2004).
[6] P. Johansson, H. Xu, and M. Käll, Phys. Rev. B **72**, 035427 (2005).
[7] M. Inoue and K. Ohtaka, J. Phys. Soc. Jpn. **52**, 3853 (1983).
[8] B. Pettinger, J. Chem. Phys. **85**, 7442 (1986).
[9] B. Pettinger, K. F. Domke, D. Zhang, R. Schuster, and G. Ertl, Phys. Rev. B **76**, 113409 (2007).
[10] M. Moskovits, Rev. Mod. Phys. **57**, 783 (1985).
[11] T. Itoh, K. Hashimoto, and Y. Ozaki, Appl. Phys. Lett. **83**, 2274 (2003).
[12] T. Itoh, K. Hashimoto, A. Ikehata, and Y. Ozaki, Chem. Phys. Lett. **389**, 225 (2004).
[13] T. Itoh, V. Biju, M. Ishikawa, Y. Kikkawa, K. Hashimoto, A. Ikehata, and Y. Ozaki, J. Chem. Phys. **124**, 134708 (2006).
[14] T. Itoh, K. Yoshida, V. Biju, Y. Kikkawa, M. Ishikawa, and Y. Ozaki, Phys. Rev. B **76**, 085405 (2007).
[15] T. Itoh, Y. Kikkawa, V. Biju, M. Ishikawa, A. Ikehata, and Y. Ozaki, J. Phys. Chem. B **110**, 21536 (2006).
[16] P. Lee and D. Misel, J. Phys. Chem. **86**, 3391 (1982).
[17] The equation we wrote in our paper is essentially the same as that of Refs. 5 and 6 although the notation was changed. By replacing $1/M_d^2$ in Refs. 5 and 6 with quenching factor q and M^4 (M is the amplification of EM factor) in Refs. 5 and 6 with M_1M_2 (M_1 and M_2 are the intensity of EM factor), Eq. (4) is obtained.
[18] C. Sonnichsen, T. Franzl, T. Wilk, G. von Plessen, J. Feldmann, O. Wilson, and P. Mulvaney, Phys. Rev. Lett. **88**, 077402 (2002).
[19] V. M. Shalaev, E. Y. Poliakov, and V. A. Markel, Phys. Rev. B **53**, 2437 (1996).
[20] T. Klar, M. Perner, S. Grosse, G. von Plessen, W. Spirkl, and J. Feldmann, Phys. Rev. Lett. **80**, 4249 (1998).
[21] M. Futamata, Y. Maruyama, and M. Ishikawa, J. Phys. Chem. B **107**, 7607 (2003).
[22] P. Matousek, M. Towrie, and A. Parker, J. Raman Spectrosc. **33**, 238 (2002).
[23] R. C. Maher, J. Hou, L. Cohen, E. Ru, J. Hadfield, J. Harvey, P. Etchegoin, F. Liu, M. Green, R. Brown, and M. Milton, J. Chem. Phys. **123**, 084702 (2005).
[24] J. Ferraro, K. Nakamoto, and C. Brown, *Introductory Raman Spectroscopy*, 2nd ed. (Elsevier, San Diego, 2003).
[25] H. Okamoto, T. Nakabayashi, and M. Tasumi, J. Phys. Chem. A **101**, 3488 (1997).
[26] T. Okamoto, I. Yamaguchi, and T. Kobayashi, Opt. Lett. **25**, 372 (2000).
[27] T. Nakamura and S. Hayashi, Jpn. J. Appl. Phys., Part 1 **44**, 6833 (2005).
[28] We calculated the spectrum of the $M_1(\lambda_L)$ factor from that of $M_1(\lambda_L)M_2(\lambda)$ in Figs. 4(d)–4(f). The calculated spectral shape of the $M_1(\lambda_L)$ factor is the same as that of $M_2(\lambda)$ from Eq. (2). Note that the wavelength of the $M_1(\lambda_L)$ maximum was set at 632 nm in Fig. 4(g)
[29] A. Otto, J. Billman, J. Eickmans, U. Erturk, and C. Pettenkofer, Surf. Sci. **138**, 319 (1984).
[30] D. Wu, J. Li, B. Ren, and Z. Tian, Chem. Soc. Rev. **37**, 1025 (2008).